Characteristics of photonic crystal fibers designed with an annular core using a single material

Shuguang Li,[1,2,*] Xiaoxia Zhang,[1] and Govind P. Agrawal[2]

[1]Key Laboratory of Metastable Materials Science and Technology, College of Science, Yanshan University, Qinhuangdao 066004, China

[2]The Institute of Optics, University of Rochester, Rochester, New York 14627, USA

*Corresponding author: lishuguang98@gmail.com

Received 23 January 2013; revised 2 April 2013; accepted 2 April 2013; posted 3 April 2013 (Doc. ID 183826); published 29 April 2013

We propose a kind of photonic crystal fiber (PCF) designed with an annular core and fabricated using a single material. Characteristics of such fibers, including the mode field distributions of both the core and cladding modes, the effective mode area of the fundamental core mode, and the dispersion profile, are investigated using the finite element method. The coupling between the fundamental mode and an excited core mode or cladding mode is discussed in order to apply the proposed design in mode-coupling devices. Results show that such a PCF may be suitable for both optical communications and optical sensing technologies. © 2013 Optical Society of America

OCIS codes: (060.0060) Fiber optics and optical communications; (060.2270) Fiber characterization.
http://dx.doi.org/10.1364/AO.52.003088

1. Introduction

Optical fibers with an annular core have been investigated in recent years because of their unique model properties. Since such fibers can provide an adiabatic mode transformation to conventional solid core fibers, they have found many device applications in short-haul and long-haul optical communication systems [1]. Hollow optical fibers (HOFs), composed of a central air hole inside a GeO_2-SiO_2 ring core and a SiO_2 cladding, are typical of optical fibers with an annular core. A mode converter based on a tapered HOF was proposed to reduce the differential modal delay penalty in optical transmission over multimode fibers [2]. A short HOF played an important role in a tunable all-fiber band-pass filter [3]. With novel core mode blocking in the HOF and an optimal design, the device showed a low insertion loss of 1.5 dB and broadband tuning range of 84.3 nm. HOFs can also be used for dispersion compensation [4] or for realizing high birefringence [5]. In the field of atomic physics, HOFs have been used to guide atoms as well [6].

Photonic crystal fibers (PCFs) have attracted much attention since they were first fabricated in 1996 [7]. A set of extraordinary optical properties can be achieved in these fibers by varying the size and arrangement of air holes in the cladding. Several kinds of PCFs based on HOF structure have been proposed in recent years [8,9]. For example, a PCF design in 2005 showed uniform and high birefringence over a wide spectral range and single polarization single-mode guidance along with a flat negative chromatic dispersion [8]. Another PCF, whose defect section consisted of a central air hole with a germanosilicate ring surrounding it, the same as in HOF, showed a large-area annular mode profile, low splice losses, and chromatic dispersion with a low slope [9]. However, these fibers needed doping of another material in the silica ring core to achieve an annular mode with excellent properties.

In this paper, we propose a PCF with an annular core that can be fabricated using a single material. Using the finite element method (FEM), basic characteristics of the fiber, including the effective mode

1559-128X/13/133088-06$15.00/0
© 2013 Optical Society of America

area and dispersion profile, are investigated and compared with an ordinary PCF designed with the same structure parameters (but without a central hole in the core). The power fraction of light located in the center air hole of the fiber is calculated as well. We also discuss the extent of coupling between the fundamental mode and an excited mode in either the core or the cladding in view of the potential applications of such fibers in optical devices. Such fibers can also be used for generating a hollow beam useful in the case of optical tweezers.

2. PCF Structure and Numerical Method

The PCF structure proposed in this paper is shown in Fig. 1. The air holes are all arranged in the shape of a hexagon. Pure silica is the only used material, and its refractive index is obtained from the Sellmeier equation. Since PCFs with similar structures have been made before, we believe that fabrication of this fiber is not difficult. Even though our structure is superficially similar to a hollow-core fiber, it differs from it in two ways. First, the second layer of air holes is missing, resulting in an annular core. Second, air holes in the fourth layer of are much smaller compared to other layers. As a result, light is transmitted in the annular core through total internal reflection, and not by the photonic bandgap effect. The diameter of the central air hole is $d0 = 1.2$ μm. Diameters of other air holes in the cladding are $d1 = 0.8$, $d2 = 0.4$, and $d3 = 0.8$ μm, respectively. The air hole pitch $\Lambda = 1.5$ μm.

The fabrication of PCFs with three different sizes of air holes would require attention to many details, Most important among them is the requirement that the relative sizes of air holes be maintained when PCF is drawn from a suitably designed preform. Since the hole sizes of our design (0.4, 0.8, and 1.2 μm) are quite dissimilar from each other, fabrication of a PCF based on our design should not be too difficult. We can use die-cast method [10] for the fabrication of PCFs that are designed in this paper. Compared with the capillary stacking method, this method can sufficiently prevent distortion of the hole shape and size in the preform when drawing fiber at a high temperature, and it can also yield a PCF without interstitial spaces. This method can prevent air holes from collapsing due to the surface tension of glass, which can result in defects in the fiber.

The FEM is employed in this paper to study numerically the optical characteristics of the fiber structure shown in Fig. 1. This method can deal with fibers of arbitrary structure by dividing a cross section of the fiber into many triangles. Maxwell's equations are then discretized for each triangular element, leading to a set of elementary matrices. A combination of such matrices creates a global matrix system for the entire structure, which is used to find the effective index and the spatial distribution of all modes numerically [11]. An anisotropic perfectly matched layer was employed at the boundary of the computational domain.

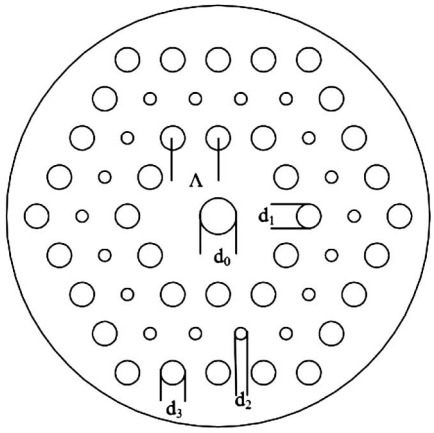

Fig. 1. Our proposed PCF structure.

3. Fiber Modes and Their Properties

A. Mode Field Distribution

Using the FEM, the field distributions of guided modes in the PCF at the 1.55 μm wavelength are shown in Fig. 2. White arrows indicate the orientation of the electric field for each mode. The top two rows show the four core modes: (a) HE11 mode, (b) TE01 mode, (c) HE21 mode, and (d) TM01 mode. Note that TE01, TM01, and HE21 are antisymmetric modes, while HE11 is a symmetric mode. All the guided core modes in this fiber have an annular distribution. To be precise, they are in a shape of hexagon (due to the core shape). Our PCF could be used for generating hollow beams, which are quite helpful for optical tweezers. The bottom two rows of Fig. 2 show the cladding modes of our fiber: (e) TM02, (f) HE22, (g) TE02, and (h) HE12 modes. As before, TM02, TE02, and HE22 are antisymmetric modes, while HE12 is a symmetric mode. The nature of coupling between the fundamental mode and another mode either in the core or the cladding will be discussed in a later section.

In air–silica optical fibers, the amount of light in the air hole is one of the important parameters to estimate the evanescent wave interaction. We have calculated the power fraction of light in the central air hole of the PCF. For a particular fiber mode, the power fraction of light f can be expressed as

$$f = \frac{\int_{\text{air}} (E_x H_y - E_y H_x) \mathrm{d}x\mathrm{d}y}{\int_{\text{total}} (E_x H_y - E_y H_x) \mathrm{d}x\mathrm{d}y}, \tag{1}$$

where E_x, E_y and H_x, H_y are the electric and magnetic field components of the mode, respectively.

The power fraction f for the fundamental HE11 mode of the PCF as a function of wavelength is shown in Fig. 3. At the telecommunication wavelengths near $\lambda = 1.55$ μm, the value of f is $<1\%$. This low power fraction indicates strong confinement of the fundamental mode within the annular core and suggests strongly that this PCF could generate a dark hollow beam that can be useful for optical tweezers.

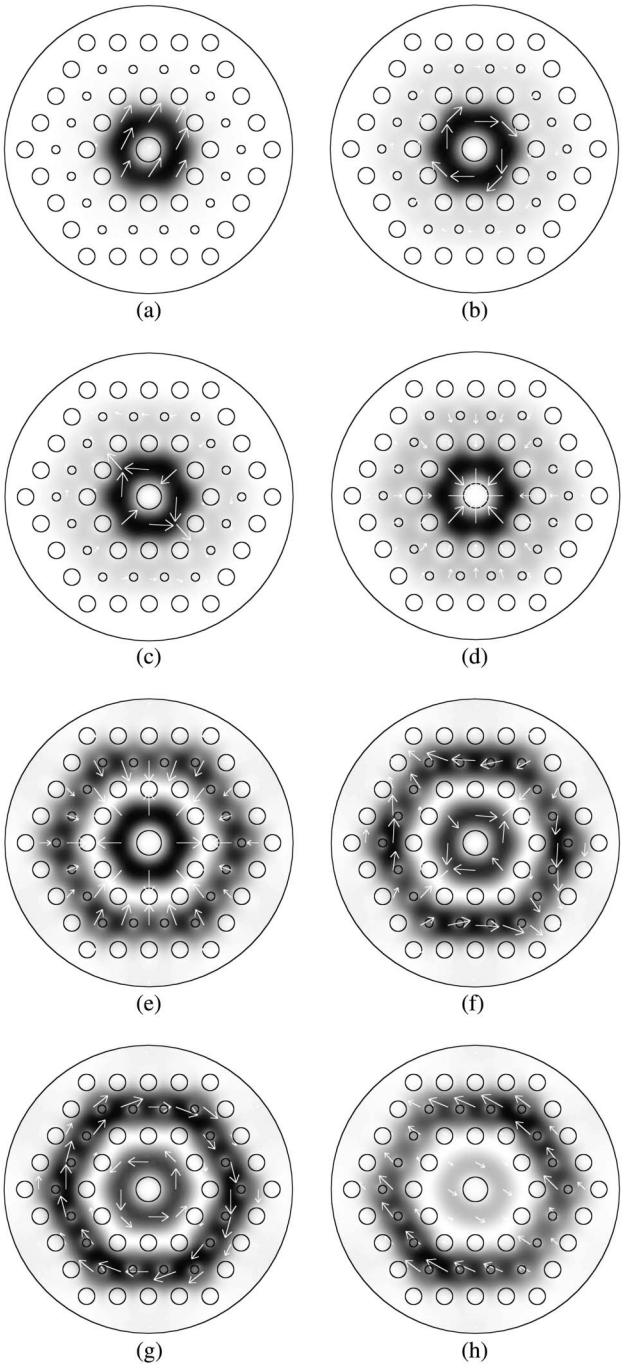

Fig. 2. Mode field distributions in the PCF at a wavelength of 1.55 μm. The top two rows show the core modes: (a) HE11, (b) TE01, (c) HE21, and (d) TM01. The bottom two rows show the cladding modes: (e) TM02, (f) HE22, (g) TE02, and (h) HE12.

B. Effective Mode Area

The effective mode area of the PCF for nonlinear effects is calculated using its standard definition [12]:

$$A_{\text{eff}} = \frac{\left(\iint F(x,y)^2 \mathrm{d}x\mathrm{d}y\right)^2}{\left(\int F(x,y)^4 \mathrm{d}x\mathrm{d}y\right)}, \tag{2}$$

where $F(x,y)$ represents the distribution of the fundamental mode field. This quantity is shown in Fig. 4 as a function of wavelength by the solid curve. The effective mode area of an ordinary PCF with the same structure but without an air hole (see the two insets) is shown by the dashed line in Fig. 4 as well.

It is clear from Fig. 4 that the effective mode area of the PCF with a central air hole is considerably larger than that of the ordinary PCF. This is expected since the central air hole spreads the mode field to the whole annular core, whereas the mode field in the ordinary PCF is confined to the fiber center. At wavelengths near 1.55 μm, the effective mode areas of the two fibers are 18.1 and 11.6 μm^2, respectively.

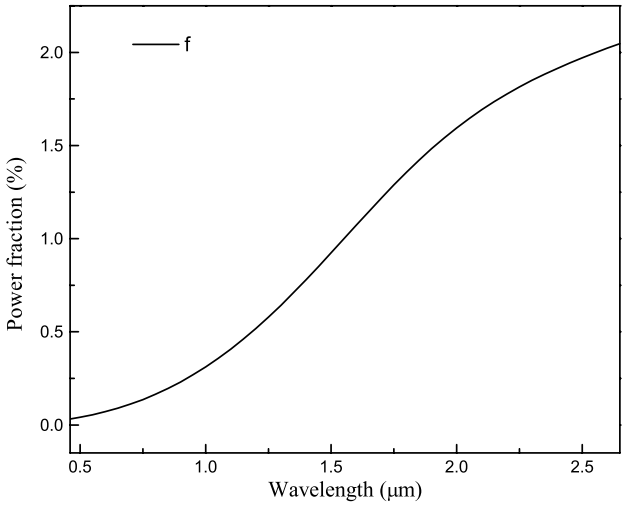

Fig. 3. Fraction of power of the fundamental mode within the central air hole plotted as a function of wavelength.

C. Dispersion

During the following dispersion calculations, we have included the wavelength dependence of the material refractive index. The total dispersion is obtained by using

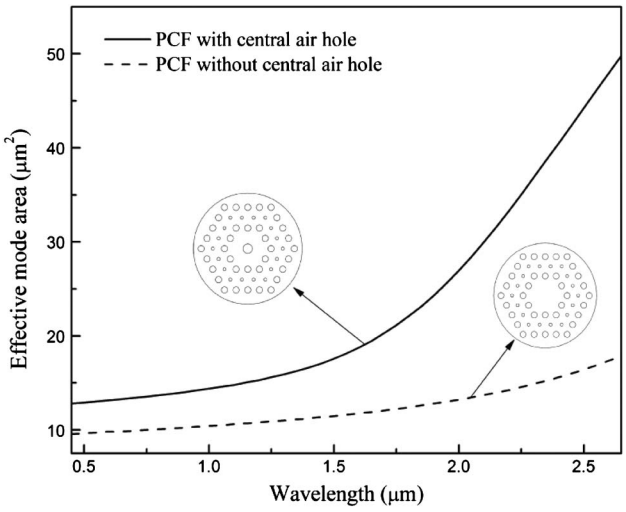

Fig. 4. Effective mode area as a function of wavelength for two PCFs designed with (solid) or without (dashed) a central air hole (see insets for the design).

$$D = -\frac{\lambda}{c}\frac{d^2\,\mathrm{Re}(n_{\mathrm{eff}})}{d\lambda^2}, \tag{3}$$

where c is the velocity of light and $\mathrm{Re}(n_{\mathrm{eff}})$ is the real part of the effective refractive index.

Figure 5 shows the dispersion profile of the four PCFs by plotting D as a function of wavelength. The solid curve in this figure represents the PCF with a central air hole. This PCF has two zero dispersion wavelengths (ZDWs) located at 0.96 and 1.45 μm, respectively. Such a fiber can be quite useful for supercontinuum (SC) generation where two ZDWs are often helpful. Notice that only one ZDW appears in the PCF at 1.02 μm, and the central air hole is absent in the PCF, (as the dashed curve shows). Notice also that our PCFs have flat dispersion in a wide wavelength region from 1.2 to 2.2 μm. PCFs with flattened dispersion find wide applications in wavelength division multiplexing, optical parametric amplification, and broadband wavelength conversion.

It is well known that the dispersion of a PCF mainly depends on the air holes that are closest to the core. In previous work, efficient dispersion control has been realized using PCFs with a central air hole [13,14]. In our work we have also changed the diameter of the central air hole to observe variations in fiber dispersion. When the air hole diameter is reduced to 0.8 μm, the two ZDWs move toward the longer wavelengths (the dashed dotted curve in Fig. 5). However, when the air hole diameter is reduced to 0.4 μm, one of the ZDWs disappears as the dotted curve shows. All four PCFs present a high negative value of D (normal dispersion) in the visible region.

D. Mode-Coupling Characteristics

PCF devices based on mode coupling are of considerable interest. For example, an all-PCF interferometer was developed in [15] by invoking interference between the core and the cladding modes of a PCF. Applications of such an interferometer as a strain sensor were demonstrated in [16]. The primary principle behind such mode-coupling devices lies in the phase matching condition [17]:

$$\beta_0 - \beta = \Delta\beta = \frac{2\pi}{L}, \tag{4}$$

where β_0 and β are the propagation constants of the fundamental mode and the other mode involved and L represents the pitch of the periodic perturbation caused by an acoustic wave or an index grating.

Before studying the mode-coupling characteristics of our PCF, we first calculate the effective refractive index n_{eff} of various guided modes of the fiber. Results are shown in Fig. 6. Figure 6(a) depicts n_{eff} of the core modes as a function of wavelength. One can see that each mode is separated by at least 6.0×10^{-4} from the others. For conventional fibers, these curves would be indistinguishable on the scale of this plot. Figure 6(b) shows n_{eff} of several cladding modes in the PCF. In the longer wavelength region,

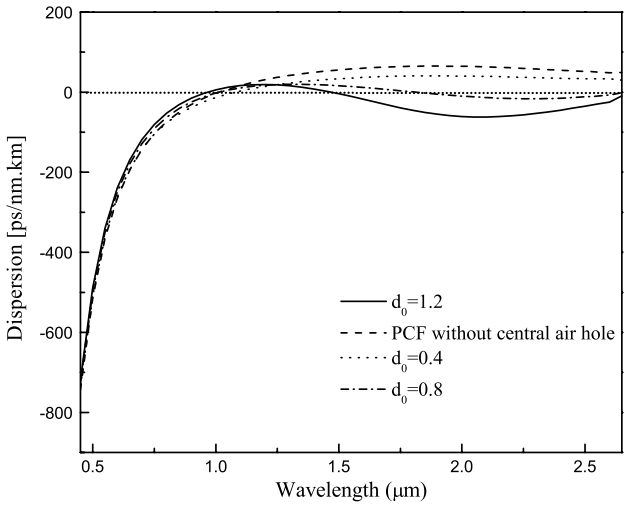

Fig. 5. Dispersion parameter D as a function wavelength for the four PCFs with designs as indicated.

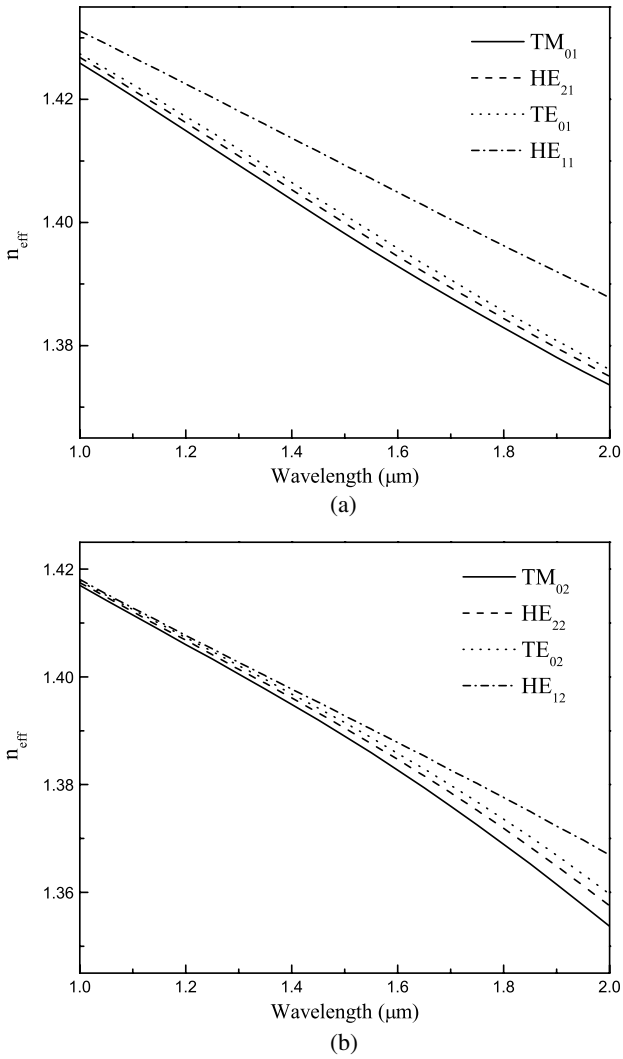

Fig. 6. Effective refractive index profile of guided modes in the PCF: (a) core modes and (b) cladding modes.

the difference in n_{eff} between two cladding modes becomes larger.

Knowledge of $\Delta\beta$ is the basis for designing mode-coupling devices. In this paper, we have calculated $\Delta\beta$ under two situations: (1) coupling of the fundamental HE11 mode to a higher-order core mode and (2) coupling of the HE11 mode to a cladding mode.

Interference between the annular core modes in PCF was first investigated experimentally in [16]. Here we study it theoretically, and results are shown in Fig. 7(a). When the HE11 mode couples to the TE01 mode, the $\Delta\beta(\lambda)$ shows a plateau with a near-zero slope in the range from 1.7 to 2.0 μm. This indicates that coupling over a very broad wavelength range (about 300 nm) can be provided by our fiber. When the HE11 mode couples to the TM01 mode or the HE21 mode, $\Delta\beta(\lambda)$ shows the shape of a parabola. At wavelength of 1.6 μm, the slopes of $\Delta\beta$, or equivalently $d\Delta\beta/d\lambda$, for the solid and dashed curves in the figure are close to zero, which could be useful for some applications [18]. Figure 7(b) illustrates the $\Delta\beta$ profile between the fundamental mode and cladding modes. In this case, $\Delta\beta(\lambda)$ between HE11 and an antisymmetric cladding mode also exhibits a parabolic shape, but it is opposite to that in Fig. 7(a). A broadband spectrum near 1.55 μm is again possible. However, the coupling between the symmetric HE11, HE12 mode shows a monotonic decease with a negative slope.

Based on the $\Delta\beta$ of the guided modes in the PCF, we have calculated the modulation pitches using Eq. (4). Results are summarized in Fig. 8. Most of the curves exhibit parabolic shapes corresponding to the results in Fig. 7. These parabolic curves in the phase matching condition will provide a relatively wide coupling bandwidth. For example, a broadband coupling is expected between 1.4 and 1.95 μm (with a bandwidth over 500 nm) for the HE11 to TM01 coupling with a periodic pitch of 140 μm. Note also that the pitch for the mode coupling between the HE11 mode and a core mode is longer than that between the HE11 mode and a cladding mode. A longer modulation pitch can ease fabrication and facilitate mass production. It also indicates robust optical characteristics against environmental perturbation [17].

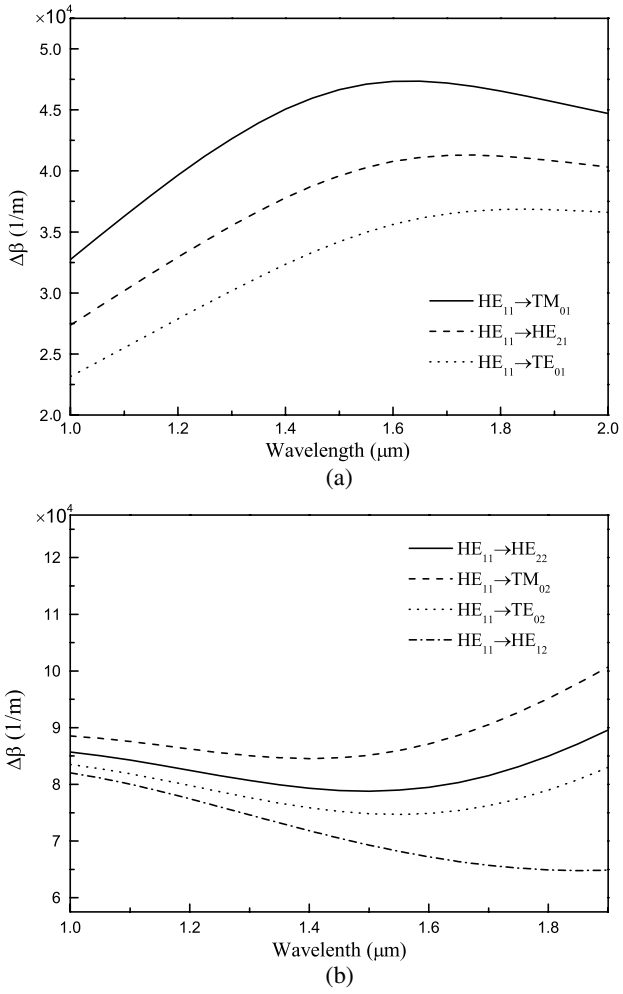

Fig. 7. Propagation constant difference between the HE11 core mode and (a) a higher-order core mode or (b) a cladding mode.

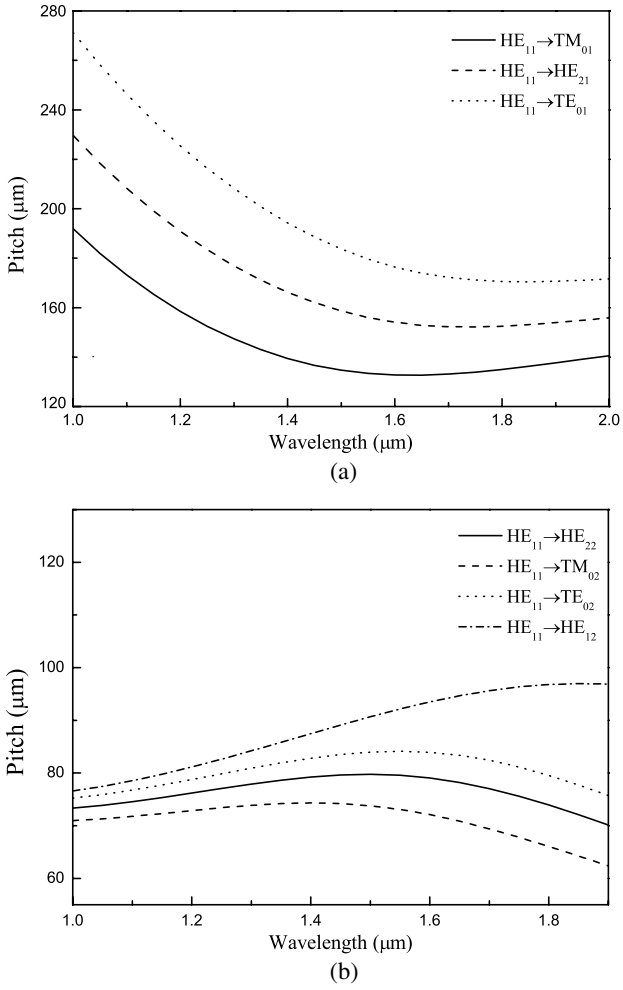

Fig. 8. Phase matching pitches for coupling between the HE11 core mode and (a) higher-order core modes and (b) cladding modes.

4. Conclusions

In this paper, a new PCF design with an annular core is proposed. The proposed PCF can be fabricated using one single material. Characteristics of this fiber are investigated numerically using the FEM algorithm. We have calculated the modal field distributions of both the core and cladding modes for our PCF. A relatively small power fraction of light in the central air hole for the fundamental mode indicates strong confinement of the mode within the annular core and the potential for dark hollow beam generation. Compared to an ordinary PCF without a central air hole, our fiber presents a larger effective mode area, which may be useful for nonlinear applications. Two ZDWs of our PCF located near 0.96 and 1.45 μm indicate that this fiber may be suitable for nonlinear applications such as SC generation. Mode-coupling characteristics for optical device application are discussed in Section 3. When the fundamental HE11 mode is coupled to another core mode, the longer modulation pitch provided by the PCF could ease the fabrication of mode-coupled devices. Our research has significant applications both in the optical communications field and in optical sensing technology.

Project supported by the National Natural Science Foundation of China (Grant No. 61178026) and the Natural Science Foundation of Hebei Province, China (Grant No. E2012203035).

References

1. K. Oh, S. Choi, Y. Jung, and J. W. Lee, "Novel hollow optical fibers and their applications in photonic devices for optical communications," J. Lightwave Technol. **23**, 524–532 (2005).
2. S. Choi, K. Oh, W. Shin, C. Park, U. Paek, K. Park, Y. Chung, Y. Kim, and Y. Lee, "Novel mode converter based on hollow optical fiber for gigabit LAN communication," IEEE Photon. Technol. Lett. **14**, 248–250 (2002).
3. S. Choi, T. Eom, Y. Jung, B. Lee, J. W. Lee, and K. Oh, "Broad-band tunable all-fiber bandpass filter based on hollow optical fiber and long-period grating pair," IEEE Photon. Technol. Lett. **17**, 115–117 (2005).
4. S. Choi and K. Oh, "A new LP02 mode dispersion compensation scheme based on mode converter using hollow optical fiber," Opt. Commun. **222**, 213–219 (2003).
5. M. M. Islam, M. A. Zahid, N. B. Jamal, M. R. Parvez, and M. S. Alam, "Wavelength dependence of guiding properties in highly birefringent elliptical ring core optical fiber," J. Electr. Eng. **36**, 10–15 (2009).
6. R. G. Dall, M. D. Hoogerland, D. Tierney, K. G. H. Baldwin, and S. J. Buckman, "Single-mode hollow optical fibres for atom guiding," Appl. Phys. B **74**, 11–18 (2002).
7. J. C. Knight, T. A. Birks, P. St. J. Russell, and D. M. Atkin, "All-silica single-mode optical fiber with photonic crystal cladding," Opt. Lett. **21**, 1547–1549 (1996).
8. S. Kim, U. Paek, and K. Oh, "New defect design in index guiding holey fiber for uniform birefringence and negative flat dispersion over a wide spectral range," Opt. Express **13**, 6039–6050 (2005).
9. S. Kim, Y. Jung, K. Oh, J. Kobelke, K. Schuster, and J. Kirchhof, "Defect and lattice structure for air-silica index-guiding holey fibers," Opt. Lett. **31**, 164–166 (2006).
10. Z. Guiyao, H. Zhiyun, L. Shuguang, and H. Lantian, "Fabrication of glass photonic crystal fibers with a die-cast process," Appl. Opt. **45**, 4433–4436 (2006).
11. F. Brechet, J. Marcou, D. Pagnoux, and P. Roy, "Complete analysis of the characteristics of propagation into photonic crystal fibers, by the finite element method," Opt. Fiber Technol. **6**, 181–191 (2000).
12. G. P. Agrawal, "Nonlinear fiber optics," in *Nonlinear Science at the Dawn of the 21st Century*, P. L. Christiansen, M. P. Sørensen, and A. C. Scott, eds. (Springer, 2000), pp. 195–211.
13. K. Saitoh, N. Florous, and M. Koshiba, "Ultra-flattened chromatic dispersion controllability using a defected-core photonic crystal fiber with low confinement losses," Opt. Express **13**, 8365–8371 (2005).
14. J. Wang, C. Jiang, W. Hu, and M. Gao, "Properties of index-guided PCF with air-core," Opt. Laser Technol. **39**, 317–321 (2007).
15. H. Y. Choi, M. J. Kim, and B. H. Lee, "All-fiber Mach-Zehnder type interferometers formed in photonic crystal fiber," Opt. Express **15**, 5711–5720 (2007).
16. W. Chen, S. Lou, L. Wang, and S. Jian, "Novel modal interferometer based on ring-core photonic crystal fiber," Chin. Opt. Lett. **8**, 986–988 (2010).
17. S. Lee, J. Park, Y. Jeong, H. Jung, and K. Oh, "Guided wave analysis of hollow optical fiber for mode-coupling device applications," J. Lightwave Technol. **27**, 4919–4926 (2009).
18. A. Yariv, "Coupled-mode theory for guided-wave optics," IEEE J. Quantum Electron. **9**, 919–933 (1973).